D4.5. Intermediate WP4 scientific report

WP4 – End user of Energy and prosumers

Author: NOVA University Lisbon (UNL)

September 2023

SMARTGYSUM project has been funded by the European Commission's Horizon 2020 Programme

SMARTGYSUM project has been funded by the European Commission's Horizon 2020 Programme

SMARTGYsum has been funded by the European Union's Horizon 2020 Programme under the Grant Agreement GA 955614

The contents of this publication are the sole responsibility of UNL (NOVA University Lisbon) and do not necessarily reflect the opinion of the European Union

Versions:

Version No.	Person in charge	Institution (acronym)	Date	Comments
1	Oleksandr Velihorskyi	CNUT	18.06.2023	First template of the deliverable report
2	Joao Martins	UNL	12.09.2023	Compilation of reports from ESR's supervisors of WP4.
3	Oleksandr Velihorskyi	CNUT	30.09.2023	Minor improvements and proofreading.
4	Enrique Romero	UEX	05.10.2023	Approval and PDF creation for uploading

SMARTGYSUM project has been funded by the European Commission's Horizon 2020 Programme

Technical References:

Project Acronym	**SmartGYsum**
Project Title	Research and Training Network for Smart and Green Energy Systems and Business Models
Project Coordinator (PC)	Enrique Romero (eromero@unex.es) Universidad de Extremadura (UEX)
Project Duration	1 October 2021 – 30 September 2025

Deliverable No.	D4.5
Dissemination Level	Public
Work Package	WP4 – End user of Energy and prosumers
Tasks	
Lead Beneficiary	14 – UNL
Contributing beneficiary (ies)	CYP, TUT, USA
Data due of deliverable	01 October 2023
Actual submission date	05 October 2023

Table of Contents

List of abbreviations

BEN	Beneficiary
Dn	Deliverable (number)
DoA	Description of Action
DS	Doctoral School
ESR	Early Stage Researcher
ETN	European Training Network
GA	Grant Agreement
IRP	Individual Research Project
ITN	Innovative Training Network
MSn	Milestone (number)
MSCA	Marie Sklodowska-Curie Actions
PC	Project Coordinator
REC	Research Ethics Committee
RSC	Recruitment and Secondment Committee
WPn	Work Package (number)

1. Executive summary

The present deliverable provides the first report about the scientific activities done and main result obtained related with the implementation of IRP in WP4 of the project.

It presents the progress of each task highlighting the work done by each of the ESRs involved in this WP, and how they contributed for the objectives of the WP. WP4 (End user of Energy and prosumers) objectives are to identify and demonstrate new ways of using electric energy enabling ESS and consumption strategies using monitoring and exogenous information; to reduce energy consumption by using emergent technology as smart meters; to analyse the benefits and possibilities of cooperation between power converters and ICT in Energy Management Systems; and to identify the main energy-related behaviour change requirements necessary to engage customers in energy applications.

In addition, it underlines the challenges faced by the different parties and their impact on the main results versus the expected ones.

The ESRs associated with this WP4 are:

- ESR9 (**Cheikh Elkebir Sidi Lekhel**), coordinated by CYU. The project title is "Embedded Real-Time System for Fault Tolerant, High Reliable and Resilient Power Electronic in Prosumers Applications" and the objectives are (1) to provide an effective consumer cooperation and coordination to optimize energy production and distribution through the development of cyber-physical systems; (2) and to enhance the physical and data safety through the development of embedded real-time systems, while reducing their cost and energy requirement and reducing their vulnerability and dependency on data connections.
- ESR10 (**Pietro Emiliani**), coordinated by TUT. The project title is "Residential Energy Management Systems based on Micro AC-grid integrated Energy Storage System with online identification of parameters" and the objectives are to optimize the behaviour of buildings considered as Energy Management Systems through the integration of smart sensors and monitoring systems.
- ESR11 (**Luis Enrique Garcia Marrero**), coordinated by USA. The project title is "On-line diagnosis and optimization of Energy Management Systems for Smart Buildings" and the objectives are (1) to create the smart devices and applications needed to optimize the consumption of energy among the different parts and applications of Smart Buildings; (2) and to research in the behaviour of consumers in smart buildings to optimize the consumption of energy.

The results obtained by ESR9 thus far are helping to establish the necessary groundwork for initiating the design of the energy router supervisor. In a later phase, this supervisor will be responsible for controlling the energy flow within the residential application. Currently, a simulation model has been developed to generate realistic load profiles that vary based on the season, occupancy, and weather conditions. Additionally, the appliances have been modelled to simplify their management in subsequent phases.

The results obtained by ESR10 presents a ground-breaking modulation strategy for power converter topologies, ushering in several noteworthy advantages. The strategy achieves full-range soft-switching, ensuring efficient operation across diverse load conditions. It effectively eliminates voltage spikes in matrix side transistors, enhancing converter reliability. A quasi-resonant transient aids zero-voltage switching (ZVS) for DC side switches, reducing losses and enhancing efficiency, even at low loads. The introduction of lossless snubber capacitors further reduces DC side switch losses by limiting voltage rise rates during turn-off. Remarkably, this modulation approach enables a substantial reduction in switching frequency, with MC switches operating for just 1/6th of a grid frequency period. It ensures consistent regulation without the need for modulation scheme changes based on voltage or power level variations, offering versatility for both inverter and rectifier operations using the same hardware. Nonetheless, voltage ringing at the MC remains a challenge, suggesting potential solutions such as switch overrating or external clamping circuits. Minimizing transformer leakage inductance is recommended to alleviate ringing-related energy issues and enhance MC commutation efficiency.

The research findings of ESR11 significantly advance the workpackage goals through three key outcomes. Firstly, a Multi-Objective Formulation for Photovoltaic Module Parameter Identification enhances precision in diagnosing

photovoltaic systems, enabling efficient energy storage and consumption strategies. Secondly, the Double-Single Diode Model (D-SDM) for Parameter Identification excels under varying conditions, aiding adaptable energy strategies and building trust in energy applications. Lastly, a Real-Time NILM Technique for Low-Frequency Sampling accelerates responses to consumption events, optimizing energy usage and engaging customers through real-time feedback. These outcomes collectively contribute to the workpackage objectives, promoting efficient energy utilization and customer involvement in energy-saving practices.

1.1. Objectives of the deliverable

The objective of the intermediate scientific is to compile the results obtained in the corresponding IRPs included in the WP4.

1.2. Organisation of the deliverable

The present deliverable is based on the report made by the ESRs describing their yearly work towards the WP and Tasks objectives. Overall, the work done is in line with what was expected with some deviations, whose causes differ from case to case.

ESR09 had undergone a big challenge the previous year. The first recruited candidate did not pass the trial period and his contract was cancelled. No results were obtained during this period. A second call was launched. Considering the time allotted to the recruiting process, a new candidate was officially assigned the job in May 2023. Therefore, concerning ESR09, the focus will be on the work done during the last four months. This work mainly consisted of state of art study and definition of the application context. In contrast with the first candidate, the new ESR is diligently acquainting themselves with the subject matter, demonstrating a strong work ethic and a serious commitment to their tasks.

The ESR10's work has yielded notable outcomes, including 8 IEEE conference papers, participation in 5 workshops and symposiums, contribution to 1 book chapter, and a journal paper currently undergoing revision. Overall, the ESR10's performance is highly commendable. However, it is important to note that the ESR10s activities were temporarily halted in June 2023 at the employee's request.

Despite a delay in the ESR11 recruitment process due to a VISA issue, the IRP commenced on the ESR11's recruitment date without accumulating any subsequent delays. Progress in research activities has adhered to the expected timeline, with a primary focus on two key objectives: developing smart devices and applications essential for optimizing energy consumption within various components and applications of Smart Buildings and conducting research on consumer behaviour in smart buildings to enhance energy consumption optimization. Additionally, preliminary findings from these endeavours have been disseminated through conference papers.

2. General progress of the action

2.1. WP4 Objectives and tasks

WP4 (End user of Energy and prosumers) objectives are:

i. to identify and demonstrate new ways of using electric energy enabling ESS and consumption strategies using monitoring and exogenous information;
ii. to reduce energy consumption by using emergent technology as smart meters
iii. to analyse the benefits and possibilities of cooperation between power converters and ICT in Energy Management Systems;
iv. to identify the main energy-related behaviour change requirements necessary to engage customers in energy applications.

WP4 (End user of Energy and prosumers) tasks are:

- Task 4.1: Development of embedded real-time system to enhance the tolerance and reliability of power electronics (UNL-USA-BRIG).
- Task 4.2: Design and in-loop Residential Energy Management Systems based on microgrid integrated Energy Storage Systems (UNL-KIT-OPAL).
- Task 4.3: On-line diagnosis and optimization of Energy Management Systems for Smart Buildings (UNL-USA).
- Task 4.4: Elaboration of partial and final scientific reports (UNL)

2.2. WP4 – Workpackage progress

(Include here a summary about when each IRP started that is supposed to be the recruitment date of the ESR. Please indicate if ESR there were two ESR's in the same position in different time – in such a case please add additional row for specified ESR)

ESR	Starting date	General evaluation	Status
9	01/09/2022 – 09/01/2023	The first candidate showed lack of motivation, weakness in the required background knowledge.	Contract cancelled
9	01/05/2023 –	The new ESR is getting familiar with the subject, hardworking and serious.	On going
10	01/02/2023	The ESR's work results have been presented in 8 IEEE conference papers, 5 workshops & symposiums, 1 book chapter and 1 journal paper (currently under revision). The overall activity of the ESR can be evaluated as very good. The activities have been interrupted in June 2023 in accordance with the request of the employee.	On hold (?)
11	01/11/2022	The procedure for the ESR recruitment has been completed with some months of delay due to VISA issue. The IRP started with the recruitment date of ESR and no delay has been accumulated. The progress in the research activities is in line with the expected timetable and mainly focused on: 1) to create the smart devices and applications needed to optimize the consumption of energy among the different parts and applications of Smart Building; 2) to research in the behaviour of consumers in smart buildings to optimize the consumption of energy. Some initial results have been also published in conference papers.	In progress

3. WP4 Tasks progress

3.1. Task 4.1 – IRP9 "Edge Computing Platform for Fault Tolerant, High Reliable and Resilient Power Electronic in Prosumers Applications"

3.1.1. Introduction

As stated previously, regarding ESR09, the work consists mainly of state of art study to define the application context and to establish the background in order to move towards the objectives. The work presented hereby is obtained during 4 months in the facilities of SATIE laboratory, UMR CNRS 8029, at CY Cergy Paris University.

3.1.2. Scientific outcomes

The final objective of ESR09 is to design a supervisor for the Energy Router to control and optimize in real-time the energy flows in a residential application.

Prior to designing the Edge Computing Platform, the application itself is to be modelled. Therefore, the first step is to define the application context. The goal is to have a model that reflects the best the domestic usage of energy in a common household. The considered application is a residential house of 80 m2 with 4 inhabitants. This is chosen in compliance with the scale of the considered application in other ESR within this WP4. The house is connected to two sources: the grid (with different tariffs) and PV panels in conjunction with a battery storage system. Phase one in this work is to establish the list of main equipment/ appliances to be considered along with their operating point, operating duration, occurrence… To do so, an excessive state of art phase is done. It is based on previous work that can be found in the literature detailing appliances model (mainly for demand side management problem) as well as overviewing national statistical studies. The objective is to build an application that reflects a realistic common case with the usual daily scenarios. In addition to the commonly knows loads, a battery charger for an electrical car is included in the loads.

Based on these studies, several load profiles are generated corresponding to different seasons and occupancy criterion (working day / weekend). The loads are classified as well: base loads (always on), daily predictable loads (lighting, TV…), shiftable non-daily loads with long operating cycles, unpredictable punctual loads (microwave, coffee machine, hair dryer). As an improvement of the existing models in the literature, the developed appliance models take into account the ambient temperature for a more generic approach regarding the optimization problem.

Phase two that is in preparation focuses on the optimization of the PV-battery sizing. The aim is to choose from an economical point of view the best combination of PV panels / Batteries to fulfill the lowest overall cost (installation and running cost considering grid tariffs) over a considered period of time. Different scenarios can be considered: the PV/battery can be sized to cover the additional extra load during peak load consumption, or simply a fraction of the total demand load (20%, 50%…). The goal is to find the best combination PV/Battery for each proposed scenario and then choose the best one with the best scenario.

Prior to the optimization problem itself, some work is needed ahead: PV modeling, battery pack modelling, establishing the economic problem with all the costs. Once the PV-battery sizing phase is achieved, the optimal energy management within the application will be then attacked.

3.1.3. Contribution to the WP objectives

The results up-to day help preparing the needed background to launch the design of the energy router supervisor in order in a later phase to control the energy flow within the residential application. Today, a simulation model is developed that generates realistic load profiles that vary with the season, the occupancy, and the weather conditions. The appliances are modeled to facilitate their management in a later phase.

3.2. Task 4.2 – IRP10 "Energy Management Systems for Residential Micro-Grids with Integrated Energy Storage"

3.2.1. Introduction

ESR10 was enrolled to Tallinn University of Technology on 1 Feb. 2022. The 4-year plan have been created, consisting of the following work-packages: Analysis of realization possibilities of residential Energy Management System (EMS), Design of full SiC single-stage EMS/Energy Router and Control of single-stage EMS/Energy Router, Energy management system with ESS. During the first year, the research and studies have been conducted in accordance with the 4-year plan. The work has been conducted in Power Electronics group of Tallinn University of Technology and Real Time System Integration group of Karlsruhe Institute of Technology (Jan-March 2023), according to ESR career development plan. The research has been conducted in the area of interlink converter between ac distribution and microgrid.

3.2.2. Scientific outcomes

1. Motivation

Wide implementation of photovoltaic (PV) and battery storage systems (BESS) motivates associated developments in power electronics. Given that PVs, BESSs, and most modern loads operate with dc, dc microgrids are an attractive concept for interfacing generation, storage, and loads, providing several important advantages, such as fewer power conversion stages, higher efficiency, and higher reliability. To ensure back-up energy source and enable energy feed-in, dc microgrids can be connected to the conventional ac distribution grid, using a bidirectional dc/ac converter. This converter is typically realized with a two-stage topology: an isolated dc/dc stage that feeds a constant voltage to the dc link of an inverter/rectifier. The dc link is stabilized by capacitors, which increase system volume, weight, and cost, as well as lowering reliability. Quasi single stage or single stage topologies, like the high frequency link converter (HFLC) shown in Fig. 1, offer an attractive alternative, eliminating the dc link and providing isolation with a high frequency transformer (HFT). The dc side of a HFLC uses a voltage source full bridge converter (FBC) to feed the primary of a HFT with a high frequency ac voltage. The secondary of the HFT is connected to a one by three phase matrix converter (MC) that steps down the frequency to grid frequency.

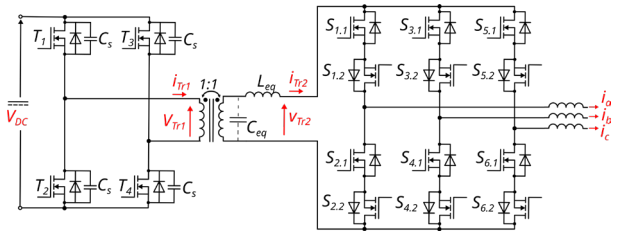

Fig. 1. Three-phase HFLC topology

2. Modulation scheme

To maintain high power conversion efficiency, switching losses should be minimized. The ac side switches can be soft switched during converter leg commutations using special modulation schemes. Still, the existing sequences have shortcomings due to complexity, duty cycle loss or limited effect. The proposed commutation sequence uses a quasi-resonance (QR) state to recharge the snubber capacitors, allowing fast zero voltage switching (ZVS) transient even at low loads. All converter switches operate under favourable switching conditions. Furthermore, at any time instant, two of the switches operate at reduced frequency. The commutation sequences can be applied for both inverter and rectifier modes of operation. No additional circuitry is required, and the control can be made quite simple.

Table I shows the MC switch behaviour for different ac side currents. "Active switches" control the power flow in the two controlled legs. The synchronous rectification (SR) switches are the ones that are in anti-series with the active switches and conduct through their body diode, they can either be left OFF or operated in SR. "Inverter Mode QR switches" initiate the freewheeling state when inverting, and are always ON when rectifying, whereas "Rectifier Mode QR switches" initiate the freewheeling state when rectifying, and are always ON when inverting. Fig. 2 gives a detailed description of the inverter operation in sector 2 during one switching period. For simplicity, SR is not considered, but

obviously it can be applied to any switch whose body diode is conducting. The leg commutation and QR transient intervals are exaggerated for clarity.

TABLE I
SWITCHING MODES

Sector	Current			Active Switches	Synchronous Rectification	Inverter Mode QR Switches	Rectifier Mode QR Switches
	a	b	c				
1	+	-	-	$S_{3.2}, S_{4.1}$ $S_{5.2}, S_{6.1}$	$S_{3.1}, S_{4.2}$ $S_{5.1}, S_{6.2}$	$S_{1.2}, S_{2.1}$	$S_{1.1}, S_{2.2}$
2	+	+	-	$S_{1.1}, S_{2.2}$ $S_{3.1}, S_{4.2}$	$S_{1.2}, S_{2.1}$ $S_{3.2}, S_{4.1}$	$S_{5.1}, S_{6.2}$	$S_{5.2}, S_{6.1}$
3	-	+	-	$S_{1.2}, S_{2.1}$ $S_{5.2}, S_{6.1}$	$S_{1.1}, S_{2.2}$ $S_{5.1}, S_{6.2}$	$S_{3.2}, S_{4.1}$	$S_{3.1}, S_{4.2}$
4	-	+	+	$S_{3.1}, S_{4.2}$ $S_{5.1}, S_{6.2}$	$S_{3.2}, S_{4.1}$ $S_{5.2}, S_{6.1}$	$S_{1.1}, S_{2.2}$	$S_{1.2}, S_{2.1}$
5	-	-	+	$S_{1.2}, S_{2.1}$ $S_{3.2}, S_{4.1}$	$S_{1.1}, S_{1.2}$ $S_{3.1}, S_{4.2}$	$S_{5.2}, S_{6.1}$	$S_{5.1}, S_{6.2}$
6	+	-	+	$S_{1.1}, S_{2.2}$ $S_{5.1}, S_{6.2}$	$S_{1.2}, S_{1.1}$ $S_{3.2}, S_{4.1}$	$S_{3.1}, S_{4.2}$	$S_{3.2}, S_{4.1}$

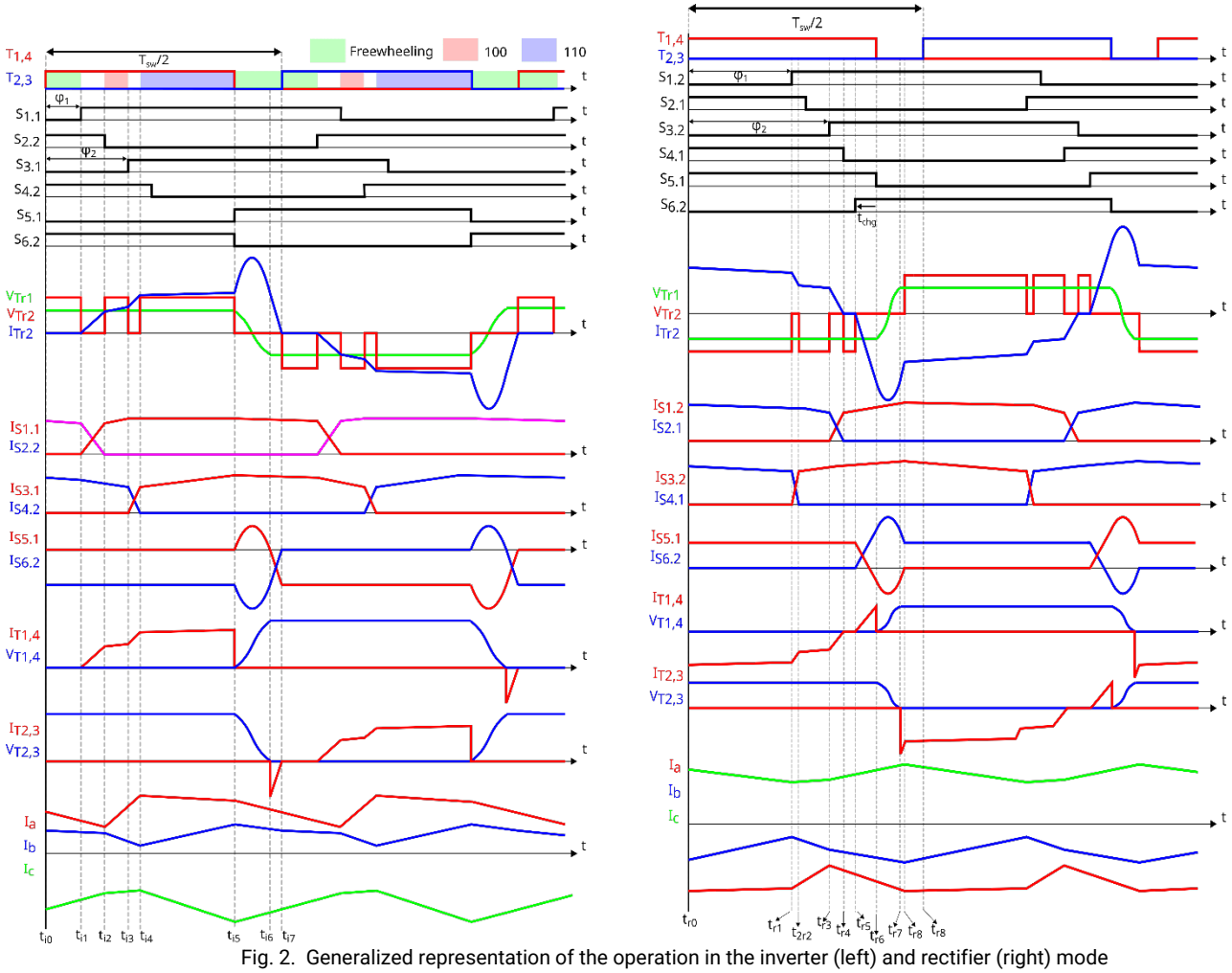

Fig. 2. Generalized representation of the operation in the inverter (left) and rectifier (right) mode

t_{i0}: The inverter is in the freewheeling state. $S_{2.2}$, $S_{4.2}$, $S_{5.2}$, $S_{6.1}$, and $S_{6.2}$ are ON. The body diodes of $S_{2.1}$, $S_{4.1}$, and $S_{6.2}$ are conducting. In the instant t_{i0} the switches T_1 and T_4 turn ON with ZVS. No power is transferred, and there is no transformer current.

t_{i1}: $S_{1.1}$is turned ON with soft-switching, shorting the leg, and the load current in leg 1 begins to redistribute from $S_{2.2}$to $S_{1.1}$, limited by the leakage inductance of the transformer.

t_{i2}: When the current has completely redistributed the body diode of $S_{2.1}$stops conducting. $S_{2.2}$can now be turned OFF with ZCS. Current begins to flow through the transformer in the positive direction and the inverter is in the active state, with configuration "100". The current through leg 1 increases.

t_{i3}: Leg 2 undergoes a process analogous to leg 1 that begins by turning ON $S_{3.1}$
t_{i4}: The current finishes redistributing in leg 2 and the inverter is now in the "110" state. It is possible to turn OFF $S_{4.2}$ with ZCS. The current through the transformer is now equal to the current in the freewheeling leg.
t_{i5}: T_1, T_4 are switched OFF, with snubber capacitors limiting the slope of the voltage. $S_{5.1}$is switched ON. The body diode of $S_{6.2}$begins conducting, shorting the secondary of the transformer. The inverter returns to the freewheeling state. The current through leg 3 increases as the QR transient takes place between the transformer leakage inductance snubber capacitors. The current through the leakage inductance of the transformer, which is now greater than the nominal current of the converter, recharges the snubber capacitors.
t_{i6}: Once the voltage across the snubber capacitors has changed its sign, T_2, T_3begin to conduct the load current through their body diodes, which decays linearly to zero, limited by the leakage inductance. The current in leg 3 redistributes from $S_{6.x}$ to $S_{5.x}$, analogous to the current redistribution in legs 1 and 2. The QR transient is shown more explicitly in Fig. 3. For simplicity only the QR leg is shown on the ac side.
t_{i7}: The transformer does not conduct any current. It is possible to turn ON T_2, T_3 with ZVS. The process can now be repeated with opposite polarity of the HFT.

Fig. 2 also shows the waveforms during a switching period of the converter operating as a rectifier. The description will be made briefer, as it is largely analogous to the inverter case.

Immediately before t_0, the rectifier is in the active state. $S_{2.1}$, $S_{4.1}$, $S_{5.1}$, $S_{5.2}$, $S_{6.1}$ are ON. The body diodes of $S_{2.2}$, $S_{4.2}$, and $S_{5.2}$ are conducting. Power is transferred through the body diodes of T_1, T_4. In the instant t_0 the switches T_1 and T_4 turn on and operate in SR.

During the FBC ON-time there are two leg commutations which redistribute current between arms of the leg, analogous to the inverter case. However, whereas the transformer current was equal to load current after the second leg commutation when inverting, it is zero when rectifying. Because of this, it is necessary to introduce an overlap in the freewheeling leg, between $S_{5.1}$ and $S_{6.2}$, in the interval $t_{r4} - t_{r5}$. During this interval the transformer current increases to match the load current. The QR transient takes place between $t_{r5} - t_{r6}$, after which the rectifier enters the active state.

Ideally, the transformer current at t_{r5} would perfectly match the load current. This is difficult to achieve precisely, as it is determined by the controlled overlap time t_{chg}, and there will be some overshoot. This introduces an additional interval $t_{r7} - t_{r8}$ during which the transformer current decays to load current after the QR transient, slightly increasing the duty cycle loss and energy circulation.

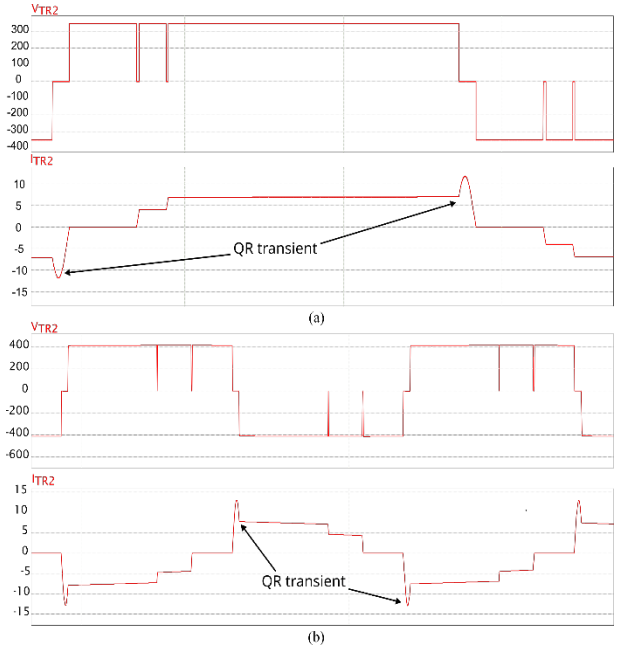

Fig. 3. Simulation transformer voltage and current during inverter mode (a) and rectifier mode (b)

Fig. 3(a) shows the voltage at the input of the MC and the transformer current during inverter operation. When a leg is short-circuited, i.e., during a the QR transient or a leg commutation, there is duty cycle loss as V_{TR2} falls to zero.

After the QR transient, the converter is in the freewheeling state with zero transformer current. Fig. 3(b) shows the same waveforms when rectifying. The converter is in the active state immediately after the QR transient and freewheeling after the second leg commutation.

Fig. 3 shows the currents through a three phase load when the converter is operating as an inverter. The phase shift was controlled with a PI loop applied to the ac side currents.

3. Space vector modulation

The space vector control of high frequency link converters is conceptually identical to that of the conventional three phase two-level inverter. The current sector imposes some constraints on possible vector sequences that allow for ZCS of the MC. The optimized sequence must ensure that these constraints are fulfilled, as well as using the vectors adjacent to the reference vector and maximizing the zero vector when used. The optimized vector sequence for space vector control was first derived for the non-isolated high frequency link inverter, shown in Fig. 4. One active voltage vector is suppressed by being placed immediately before the dc side commutation, resulting in essentially a 3 vector sequence. This suppressed vector corresponds to the clamped leg which has the highest current reference, thereby accelerating the snubber recharge process.

The voltage reference is rotated with an angle of $\Delta\theta_k = (k-1)\pi/3$, where k is the current sector, and placed in a normalized vector frame composed of V', where the corresponding real voltage vector which depends on the current sector.

Optimized 3 vector sequence in Normalized Reference Frame

	A	B1	B2	C1	C2	D	E	F1	F2	G1	G2	H
$\mathbf{V_x}$	V7'	V4'	V4'	V3'	V3'	V4'	V4'	V5'	V5'	V4'	V4'	V7'
$\mathbf{V_y}$	V2'	V7'	V3'	V0'	V2'	V3'	V5'	V0'	V6'	V7'	V5'	V6'
$\mathbf{V_z}$	V1'	V2'	V2'	V1'	V1'	V0'	V0'	V1'	V1'	V6'	V6'	V1'

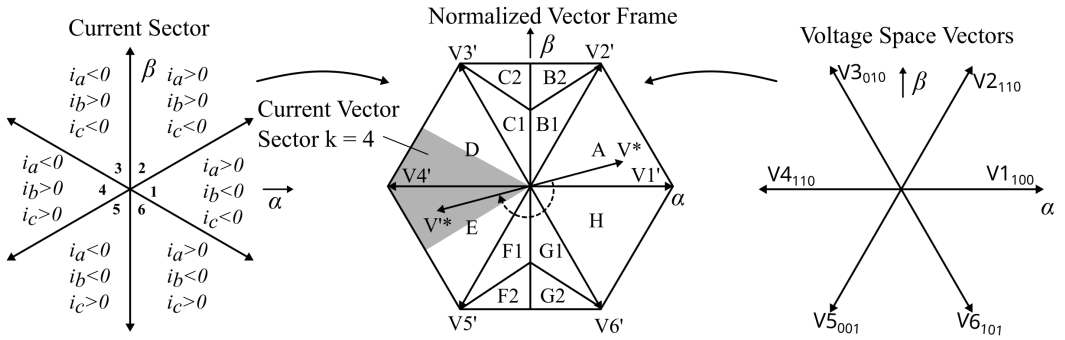

Normalized Space Vectors

	V0'	V1'	V2'	V3'	V4'	V5'	V6'	V7'
k=1	V0	V1	V2	V3	V4	V5	V6	V7
k=2	V7	V2	V3	V4	V5	V6	V1	V0
k=3	V0	V3	V4	V5	V6	V1	V2	V7
k=4	V7	V4	V5	V6	V1	V2	V3	V0
k=5	V0	V5	V6	V1	V2	V3	V4	V7
k=6	V7	V6	V1	V2	V3	V4	V5	V0

Duty Cycle Calculation

$$\begin{bmatrix}\delta_1\\ \delta_2\\ \delta_3\end{bmatrix} = \begin{bmatrix}V'_{x,\alpha} & V'_{y,\alpha} & V'_{z,\alpha}\\ V'_{x,\beta} & V'_{y,\beta} & V'_{z,\beta}\\ 1 & 1 & 1\end{bmatrix}^{-1} \begin{bmatrix}V'^{*}_{\alpha}\\ V'^{*}_{\beta}\\ 1\end{bmatrix}$$

Fig.4. Space vector modulation for selecting optimized three vector sequence. The optimal three vector sequence is determined by the region of the reference vector in the normalized space vector frame, and then the real vectors are obtained by transforming the normalized vectors according to the current sector.

The normalized zero vectors depend on the polarity of the current with highest reference value, i.e., the current with direction opposite to the other two, seen in Fig. 4. With positive current the zero vector remains unchanged whereas with negative reference the zero vectors V_0 and V_7 are exchanged.

The resulting optimal vector sequence depends on the reference voltage regions shown in Fig 4. For load angles near 0 or π radians it is always possible to use two adjacent vectors and a zero vector. On the other hand, at load angles near $\pm\pi/2$, the zero vector is either the middle vector or not used at all, however operation in these sectors is not the focus of the paper. When operating near unity power factor in inverter operation, regions A and H, the first vector is always a zero vector. Instead, rectifier operation corresponds to regions D and E wherein the last vector is always a zero vector.

After the duty cycle δ are calculated with the equation shown in Fig. 4, the real vector sequences are obtained from the current sectors, as described in Fig. 4 To reduce computational burden the inverse matrix is preloaded to a

4. Converter prototype

A 3.3 kW prototype was designed to verify the proposed topology and modulation. The design of the prototype is briefly described in the following section. An advantage of the topology is that the soft switching does not require a very precise leakage or magnetizing inductance to operate, simplifying the transformer design. At the time of this work there was still no widespread standard for dc microgrids, however 350V is a likely candidate for the voltage of the dc bus. The clamping of a leg, and use of only two adjacent voltage vectors and the zero vector extends the linear modulation range to 1.154. To account for duty cycle loss during the dc switch deadtime and leg commutations, as well as possible grid overvoltage, the transformer ratio was set at 1.82. The transformer was constructed with litz wire wound around a toroidal ferrite core. The core losses were calculated with Steinmetz equations, considering a 350 V square wave impressed from the dc side and a switching frequency of 50 kHz. The design of the grid-side inductors is quite simple, as they are low frequency inductors. Enameled copper wire was wound on an iron powder core.

The peak line-to-line voltage is 570 volts. However, the MC switches suffer from a well-known problem of resonance between the output capacitance of the switches and the leakage inductance of the transformer. Solutions typically use snubber circuits or active clamping circuits. Snubber circuits reduce the efficiency of the device, and clamping circuits increase the cost, component count, and complexity. The simplest solution is a modest oversizing of the ac side switches, from 900V class to 1200V class. The IMW120R220M1H SIC MOSFET with 1200V blocking voltage and 220mOhm on resistance was selected.

On the dc side there is no ringing problem and so 650V devices can be used. External capacitors are added to provide soft turn off, and ZVS is possible at all loads with relatively low deadtimes. Due to this, the output capacitance of the switch is of little concern as it does not have a significant impact on switching losses. C3M0120065k devices with 120 mΩ on resistance and 650V blocking voltage are selected. The switches are clipped to a forced air heatsink.

The snubber capacitor must have good performance under dc bias conditions and tolerate high ripple current. For this reason, 2 kV ceramic C0G capacitors have been chosen. To provide a good trade-off between switching loss reduction, energy circulation and duty cycle loss, a relatively small snubber capacitance value of 470pF is sufficient, given the ultra-fast switching of modern SiC MOSFETs. The prototype is controlled by a F28379D microcontroller control card.

5. Experimental results

Experiments were conducted on the prototype to verify the proposed modulation method and validity of the design. Switching waveforms were recorded to demonstrate the soft-switching transients of the converter. Finally, the converter efficiency was estimated with a Yokogawa WT1800 power analyzer.

Fig. 5 shows the QR transient that develops during the shoot-through state of the transformer at high, medium, and low power levels. The deadtime is kept at 100 ns, however, it can be optimized for different operating points. At high power levels there is enough energy in the leakage inductance to recharge the snubber capacitors, so that the QR transient is not visible. It can be seen that the voltage across the snubbers, shown in channel 2, very rapidly swings to the opposite dc rail. The voltage on the secondary of the transformer is briefly clamped to zero volts as the converter is in a shoot-through state. Noticeable ringing can be seen on the secondary of the transformer, due to unintended resonance between the output capacitance of the MC switches and the leakage inductance of the transformer.

At medium power level, shown in Fig. 5, (b) and (e), the QR state becomes noticeable. The current increases above its nominal value during the deadtime, accelerating the recharge of the snubber capacitors. The duration of the zero-voltage clamping on the secondary of the transformer increases as it takes longer for the snubber capacitors to recharge.

Finally, in the case of extremely low load, as in Fig. 5, (c) and (f), almost all of the energy to recharge the snubbers is provided by the QR transient. The secondary of the transformer is clamped for the longest time as it takes longer for the snubber capacitors to swing to the opposite dc rail, however it is still possible to achieve ZVS turn on within the 100 ns, even with almost no-load current.

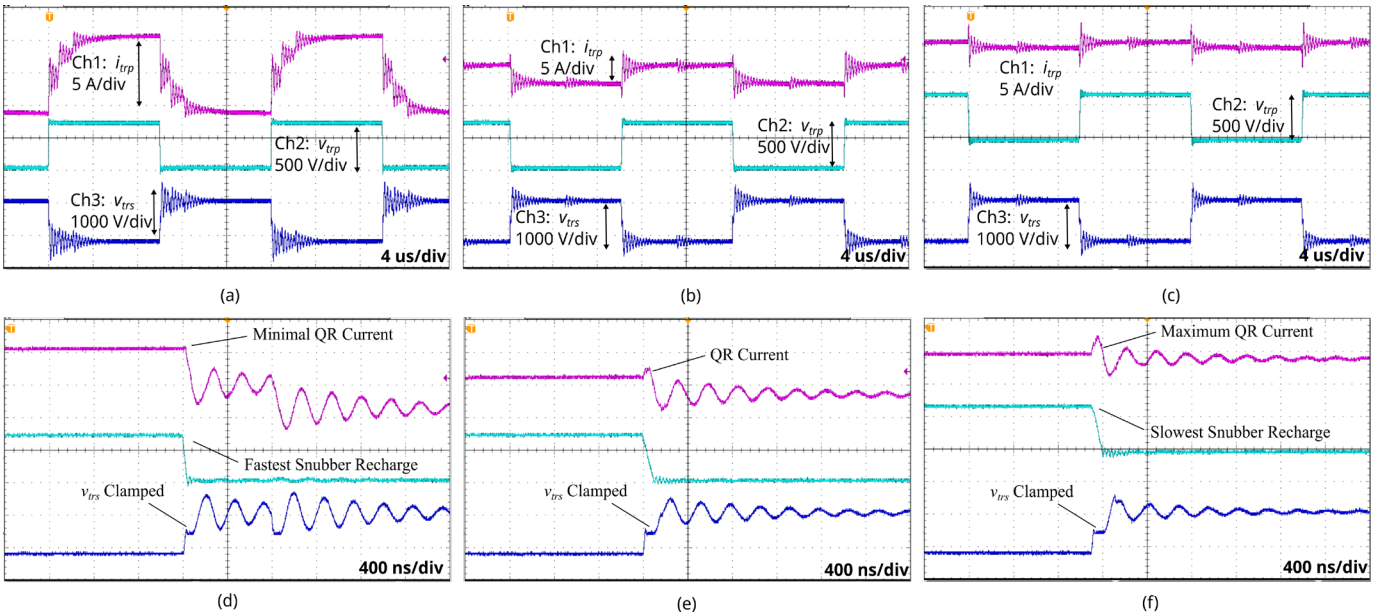

Fig. 5 The dc side ZVS turn ON and recharge of the snubbers from the QR transient under inverter operation. Channel 1 shows the transformer primary current, channel 2 shows the transformer primary voltage, channel 3 shows the transformer secondary voltage. a, b, and c, show the switching waveforms during operation at high, medium, and low power. d, e, and f are zoomed in images of the switching waveforms from a, b, and c respectively, showing the development of the QR transient and snubber recharge.

Fig. 6. shows three sinusoidal currents generated on a three-phase resistive load. When the sector changes small distortions can be observed on the output current Although the converter switching frequency is 50 kHz, the effective switching frequency seen by the inductors is 100 kHz.

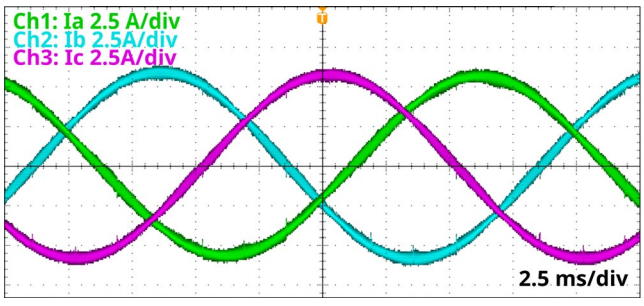

Fig. 6 Three phase currents on a resistive load with a power of 3.3 kW. Small distortions can be observed during the sector changes.

The efficiency is measured over a wide power range (Fig. 7). The full-load soft switching results in an efficiency curve that is quite flat over a wide load range. The converter maintains 89.2% efficiency at only 270 watts, equivalent to about 8% load. In this operating point it is estimated that 18.8 watts of losses, about 60% are from the transformer core static losses. The converter achieves peak efficiency at 2.2kW with an efficiency of 96.7%. At higher power levels the efficiency begins to decrease due to conduction losses.

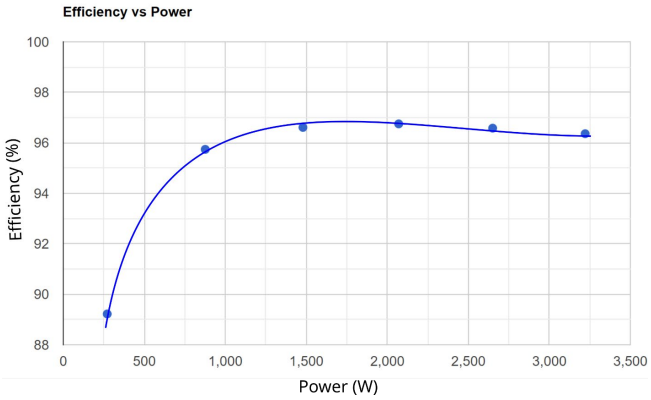

Fig. 7 Efficiency at different operating power.

3.2.3. Contribution to the WP objectives

The microgrid is typically assumed to be connected to the AC distribution system by the means of an interlink converter. This converter is responsible for the energy exchange between the distribution grid and the microgrid and needs to support bidirectional power flow. From the microgrid side the interlink converter needs to operate in conjunction with storage system and distributed generation, while simultaneously providing ancillary services for the AC distribution system. Recent standards for dc microgrids assume galvanic isolation and to solve this, two-stage systems consisting of inverter/rectifier and isolated converter are typically used.

Single-stage isolated dc-ac converters based on a three-phase high-frequency link topology are an attractive alternative to the more conventional two-stage configurations that require a dc link. Topologies with a current source MC offer reduced conduction losses and lower computational burden due to simpler modulation. The grid side inductor design is simple, and the filtering effort is reduced due to the ripple frequency of the current being twice the switching frequency. However, problems related to voltage spikes, switching losses, and modulation complexity have hindered their adoption in practical applications. Performed research contributes to further development of such topologies by presenting a modulation strategy that provides full range soft-switching and low circulating energy, allowing for high efficiency at all loads. The proposed modulation has all the advantages of previously presented solutions, with the following additional benefits:

- Voltage spikes across the matrix side transistors are avoided.
- A quasi-resonant transient provides energy for ZVS turn on of the dc side switches at all loads, reducing switching losses.
- Switching losses of the dc side switches are further reduced by lossless snubber capacitors that limit *dv/dt* rise across the device at turn off.
- The MC switches spend $1/6^{th}$ of a grid frequency period turned ON, effectively reducing the switching frequency to $5/6^{th}$ of the switching frequency.
- The method uses only the MC for regulation and does not require a modulation scheme change with variation of ac or dc voltage, or power level.
- The same underlying principle can be used for both inverter and rectifier operation with the same hardware and similar performance.

The voltage ringing problem at the MC is still present and cannot be solved exclusively by modulation. A modest overrating of the switches used in this paper is a possible solution. Otherwise, an external clamping circuit can be applied. To reduce the energy in the ringing the transformer leakage inductance should be minimized. This also helps reduce the duty cycle loss related to MC commutations, resulting in better RMS currents in the MC.

The prototype assumed further development to perform advanced energy management functions in the microgrid. To allow active phase load balancing a version with neutral wire connection is required.

3.2.4. Scientific achievements

Publications

#	Title, incl. citation information	Type	Status	DOI
1	Emiliani, P.; Blinov, A.; Peftitsis, D.; Giannakis, A.; Vinnikov, D. (2022). Reactive Power Control for Bidirectional Isolated High-Frequency Link Converter. 2022 International Symposium on Power Electronics, Electrical Drives, Automation and Motion, SPEEDAM 2022. IEEE, 372–376.	Conference	published	10.1109/SPEEDAM53979.2022.9842131
2	Emiliani, P.; Blinov, A.; Chub, A.; De Carne, G.; Vinnikov, D. (2022). DC Grid Interface Converter based on Three-Phase Isolated Matrix Topology with Phase-Shift Modulation. IEEE 13th International Symposium on Power Electronics for Distributed Generation Systems (PEDG): Kiel, Germany, 26-29 June 2022. IEEE, 1–6.	Conference	published	10.1109/PEDG54999.2022.9923256.
3	Emiliani, P.; Blinov, A.; Chub, A.; De Carne, G.; Vinnikov, D. (2022). Black Start and Fault Tolerant Operation of Isolated Matrix Converters for dc Microgrids. 48th Annual Conference of the Industrial Electronics Society (IECON 2022): Brussels, Belgium, 17-20 October 2022. IEEE, 1–5	Conference	published	10.1109/IECON49645.2022.9968735.
4	Verbytskyi, I.; Blinov, A.; Emiliani, P.; Galkin, I. (2022). Digital Control of PFC Rectifier with Combined Feedforward and PI Regulator. 48th Annual Conference of the Industrial Electronics Society, IECON 2022: 48th Annual Conference of the IEEE Industrial Electronics Society. IEEE	Conference	published	10.1109/IECON49645.2022.9968509
5	Arena, Gabriele; Emiliani, Pietro; Chub, Andrii; Vinnikov, Dmitri; De Carne, Giovanni (2023). DC Fast Charging of Electric Vehicles: A Review on Architecture and Power Conversion Technology. 2023 IEEE 17th International Conference on Compatibility, Power Electronics and Power Engineering (CPE-POWERENG), Tallinn, Estonia, Jun. 14-16, 2023.	Conference	published	10.1109/CPE-POWERENG58103.2023.10227492
6	Pietro Emiliani, Andrei Blinov, Giovanni De Carne, Gabriele Arena, and Dmitri Vinnikov (2023). Predictive Control for Isolated Matrix Rectifier Without Current Distortion at Sector Boundary. 2023 IEEE 17th International Conference on Compatibility, Power Electronics and Power Engineering (CPE-POWERENG), Tallinn, Estonia, Jun. 14-16, 2023.	Conference	published	10.1109/CPE-POWERENG58103.2023.10227405
7	Parham Mohseni, Pietro Emiliani, Oleksandr Husev, Dmitri Vinnikov, and Laurens Mackay (2023). A Comparison between Three-Phase Conventional Two-Stage AC-DC and Single-Stage Matrix Converter Approaches. 2023 IEEE 17th International Conference on Compatibility, Power Electronics and Power Engineering (CPE-POWERENG), Tallinn, Estonia, Jun. 14-16, 2023	Conference	published	10.1109/CPE-POWERENG58103.2023.10227438
8	Pietro Emiliani, Andrei Blinov, Giovanni De Carne, Gabriele Arena, and Dmitri Vinnikov (2023). Three-Phase Four Wire High-Frequency Link Converter for Residential DC Grids. 2023 IEEE 17th International Conference on Compatibility, Power Electronics and Power Engineering (CPE-POWERENG), Tallinn, Estonia, Jun. 14-16, 2023.	Conference	published	10.1109/CPE-POWERENG58103.2023.10227416
9	Blinov, A.; Roasto, I.; Chub, A.; Emiliani, P.; Vinnikov, D. (2023). Electric Power Management and Control in DC Buildings — State-Of-The-Art and Emerging Technologies. In: Power Quality: Infrastructures and Control. (67–96). Springer. (Studies in Infrastructure and Control).	Book chapter	published	10.1007/978-981-19-7956-9_3.
10	Three Phase Bidirectional Isolated dc/ac Matrix Converter with Full Range Soft Switching	Journal	In review	N/A

3.3. Task 4.3 – IRP11 "On-line diagnosis and optimization of Energy Management Systems for Smart Buildings"

3.3.1. Introduction

It is well known that the building sector is responsible for much of the electricity consumption and greenhouse-gas emissions in industrialized countries. In this sense, the Electric Energy System needs to adapt its structure to meet the challenges of the energy needs of the green economy, which requires a smart use and green production of energy [1]. Residential photovoltaic (PV) panels and energy storage systems (ESS) represent a promising solution in a building's microgrid [2].

Currently, new features in a building's microgrid add many possibilities for control and management. Some of these new features include advanced smart metering, demand-side management systems, and communication infrastructure providing real-time information for all system variables [3]. The utilization of data collected from smart meters has shown substantial benefits in various aspects of grid operation and maintenance, including fault detection, load forecasting, and demand response. In this sense, the analysis of detailed consumption power data is expected to enhance previously mentioned benefits and will play a critical role in the success of smart grid implementations [4].

In this research project, a building integrating a PV system and a centralized ESS will be taken as the object of study. The Energy Management System (EMS) should be able to control the ESS and suggest electrical appliance scheduling for each apartment in response to the dynamic price signals and the change of input data from various sources (smart meters, PV monitoring system, PV production), in order to determine the best operation schedule to achieve a trade-off between user comfort and energy cost. Because PV rooftop installations have limited access for inspection and maintenance, a fault diagnostic method for these systems is compulsory to avoid potential faults.

The EMS should monitor online the health of the PV system in order to notify the user when it is necessary maintenance in the system or even replace some panels. Comprehending the power consumption patterns of electrical appliances within a household is a crucial element that empowers residents to make wise and well-informed decisions. For that reason, the EMS should allow end users to monitor in near real-time the power consumption of a group of appliances. The EMS should also be able to run online on an embedded system. In these two last requirements are focused the scientific outcomes obtained in this period, that were achieved during 11 months in the facilities of the Department

3.3.2. Scientific outcomes

The results achieved so far are focused on the following expected results:

1. A novel technique to monitor online the state of health of the PV system during normal operation in order to alert the user about anomalies in the system (partial shading, the necessity of maintenance, degradation, etc). In this sense, the EIS technique will be employed to complement static and dynamic model-based approaches for diagnosing the PV device.
2. A novel NILM technique that is computationally efficient and robust. The technique should provide feedback to the user as near as possible to the real events in the building (near real-time capabilities). The algorithm should be simple and efficient enough to be implemented in an embedded system with low computational capabilities. The performance of the method shall not deteriorate drastically as the subset of monitored appliances or the subset of not monitored appliances changes in the building. The method should not involve significant occupant efforts for algorithm training.

Related to the PV diagnosis technique (Expected result 1), it is proposed and evaluated a multiobjective formulation for parameter identification in photovoltaic modules, that complement static and dynamic models (EIS technique) searching for accuracy and reliability [5]. By exploiting the dependency of common parameters between the two models, the fitting problem is transformed into a multi-objective optimization problem, which is solved using evolutionary algorithms. The results showed that selecting a tradeoff solution from the obtained Pareto front leads to a more consistent set of parameters for each environmental condition analysed [5].

The method proposed in this work is evaluated on the data obtained in the experimental campaign developed in the framework of [6]. Here, the EIS data is acquired in outdoor conditions at the MPP point. The corresponding I-V curve is also measured. The experiments account for operating states at different environmental conditions varying from medium to high irradiance. The reader can refer to [6] for more details on the experimental data. In the first step, the static objective function f1 and dynamic objective function f2 were optimized independently. The corresponding values for the best fitting allowed us to make a couple of important observations. First, the values of the series resistance of static model Rs are significatively different from the values of the series resistance of dynamic model R0; which suggests that even though these results are the best in terms of fitting error, they are not suitable for modeling the behavior of the PV module. Second, the values of the parallel resistance Rsh tend to the upper bound of the search interval in some experiments, which also suggests that the results are not consistent if compared with the other environmental conditions. Third, the constant of the modulo C is considerably different among experiments, when it is supposed to be more or less stable since it is referring to the same PV panel.

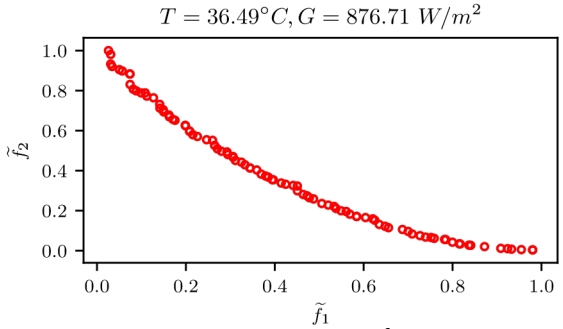

Fig. 8: Normalized Pareto front

In order to provide the decision-maker with a set of optimal tradeoff solutions, from which to choose the preferred solution, the functions f1 and f2 are optimized in a multi-objective fashion subject to the physical constraint of Rs = R0. The resultant Pareto front is shown in Fig. 8 for one experiment. It can be appreciated from Fig. 8 the uniformity of the solutions obtained along the objective domain. This behavior is very important for the decision-maker because it provides a visual representation of the trade-offs between different objectives. For selecting one solution from the PF, the goal programming method is implemented. From the results obtained in this case, was appreciated that the limitations found for the independent fitting in different environmental conditions are remediated considerably. The values of Rsh are not anymore in the boundary of the interval, also the values of C and the ideality factor n were more stable among experiments as expected. These results were presented in the INTERNATIONAL CONFERENCE ON COMPATIBILITY, POWER ELECTRONICS, AND POWER ENGINEERING (CPE-POWERENG 2023).

Also in line with the expected result 1, but devoted to obtaining reliable and coherent characterization under non-uniform operating conditions, it is proposed a Double - Single Diode Model (D-SDM) (two SDM models in series). This method relates the parameters between the resulting two SDMs circuits to obtaining reliable and coherent characterization for different irradiance conditions. A robust procedure was developed for estimating its parameters and evolutionary algorithms were employed to solve the optimization problem. The proposed methodology was also validated using experimental data from a single cell of the same type as the module [7].

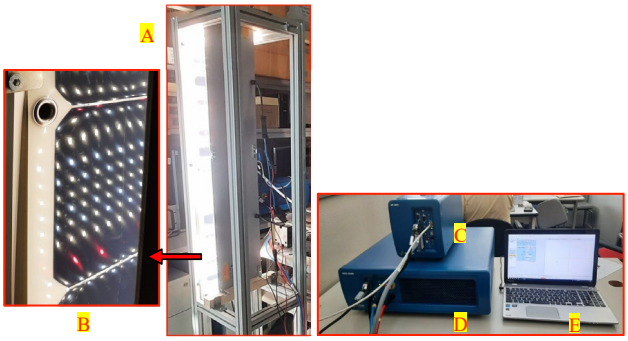

Fig. 9: Facilities for I–V curve characterization under controlled irradiance conditions
(a) PV module illuminated using a LED matrix (b) Instrument used to measure the I–V curves

Fig. 9a(A) shows the structure realized for analyzing the PV module under controlled irradiance conditions. A matrix composed of LEDs with different wavelengths is mounted in front of the PV module. The LEDs are allocated to have a uniform distribution but, due to the fact that is not possible to have a large LED surface with a single matrix, four matrices have been connected in series to cover and illuminate the full PV module. Unfortunately, the edges of the aluminum plates hosting the LEDs have some empty spaces, in such a way there are small areas with lower irradiance, leading to a non–uniform illumination among the PV cells. This is also visible in the zoom shown in Fig. 9a(B) where the LED positions are reflected on the PV module surface. The I–V curve tracer consists of (see Fig. 9b):

C – Biologic SP-200: Control unit, also able to perform the impedance spectroscopy of the device under test (however this functionality is not used in the experiments discussed in this paper).
D – Biologic HCV-3048: Amplification power stage, that operates with a current up to 32 A and a voltage up to 48 V.
E – Personal Computer: It is required to execute the BioLogic EC-Lab® Software, used to configure the experiments and for data visualization and storage.

The equipment could be used to trace I–V curves of a single PV cell (used to have reference values for some parameters without the presence of mismatch) or for a small PV module. All the measurements have been done over a commercial PV module manufactured by Solbian with reference Flex–SP50L. It is composed of 16 pseudo square back–contact mono–crystalline Silicon cells, all connected in series. Three Pt100 RTD sensors are used to measure the average temperature by means of a three-wire scheme in order to minimize the error due to voltage drop in the cables. The RTD sensors, inside silicone capsules adhered to the back surface of the module, are located in the center of three selected cells. The outputs of these sensors are connected to a Yokogawa MV1000 data logger, also connected to the personal computer.

For the SDM parameters identification, the accuracy of the fitting results for this module was not as high as expected for controlled conditions, and the fitted curves showed deviations from the experimental measurements, mainly visible around the MPP zone. Also, some of the parameters identified for the fitting procedure, in particular, the ideality factor and the parallel resistance, were on the boundary of the search interval, indicating that the SDM may not be well-suited for this I–V experimental curve and the corresponding parameters are not more realistic from the physical point of view. To further investigate the source of the observed inaccuracies in the fitting results, we conducted additional analyses with experimental data from a single cell of the same type as the module, where mismatch is not possible. In this case, by fitting several experimental curves in different irradiance conditions is possible to evaluate the capabilities of the optimization algorithm to determine reliable parameters for the SDM in uniform conditions. Additionally, single–cell experiments allow us to determine the behavior of the model parameters under different temperature and irradiance conditions, providing insights into the module's behavior under uniform conditions.

The results for different operating conditions show in this case a good fitting for the single cell. Both visually matching and fitting errors indicate that in this case, the SDM was capable of fitting the experimental curve. Also can be observed the capabilities of the algorithm to find reliable and stable parameters that remained within the expected range. To address the modeling issue, we introduced the D-SDM model with the aim of accurately characterizing the behavior of the module under varying operating conditions. We then used the same fitting algorithm as before to obtain the parameters of the D-SDM model. In this case, the fitting error decreased significantly when using the D-SDM model compared to the SDM. This decrease in error confirms the presence of mismatching in the module and validates the use of the D-SDM model to account for it in modules without bypass diode.

Fig. 10 shows a comparison of the experimental data and the calculated values obtained from the fitting procedure. It can be appreciated how the estimated values closely match the experimental data in all the points, in contrast with the results obtained using the SDM. By looking at the estimated parameters it can be appreciated that there exists a coherence among different operating conditions. This result indicates the reliability of the identified parameters and the effectiveness of the proposed model in accurately capturing the behavior of the module. It should be emphasized that the model described in this work has potential applications in addressing various forms of mismatch phenomena, such as degradation and aging effects. However, conducting further experiments under those specific conditions is essential to accurately identify the strengths and limitations of this model. These results were presented at the 8th International Conference on CLEAN ELECTRICAL POWER (ICCEP 2023). Also in line with the expected result 1, in the

same conference was presented a collaboration [8], where the main contribution was related to the development and implementation of evolutionary algorithms for parameters identification of dynamic models for PV panels.

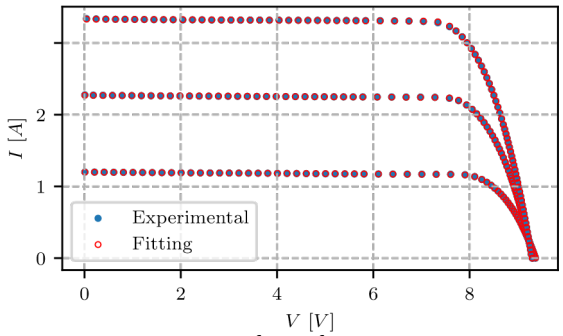

Fig. 10: D-SDM fitting for the module

In relation to the NILM technique (expected result 2), a real-time framework is proposed for low-frequency sampling. The design of the framework is based on the requirement of a real-time computationally efficient (execution time and storage) algorithm. Additionally, the framework accounts for the possibility of unknown loads causing the events in the building. The proposed NILM framework comprises three modules: Edge Detection and Base Load Detection, State Probabilities Update, and State Probabilities Tuning. The low-level architecture is composed of the three-point edge detection method, a proposed base-load detection algorithm, an update phase based on Bayes theorem, and a tuning phase based on a modified Population-Based Incremental Learning algorithm (PBIL) [9].

As shown in Fig. 11, the framework operates by receiving the aggregated power reading in the current time step. The design of the framework is based on the requirement of a real-time computationally efficient (execution time and storage) algorithm. Moreover, it optionally leverages information about the transition probabilities. Although the availability of transition probabilities is not mandatory for the functioning of the algorithm, it is expected to enhance its accuracy. Additionally, the framework accounts for the possibility of unknown loads causing the events in the building, incorporating the likelihood of the edge belonging to an unknown load and the probability of the presence of unknown loads. The proposed NILM framework comprises three modules:

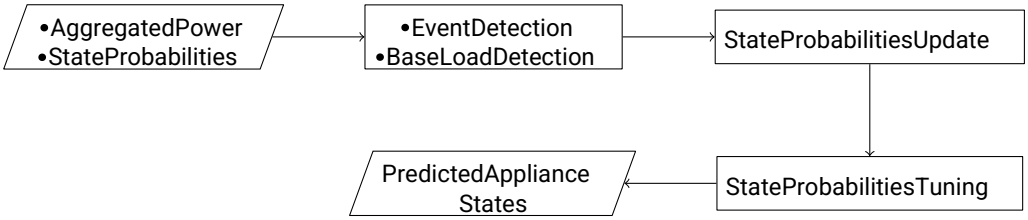

Fig. 11: Flowchart for the real-time NILM framework

Module 1: Edge Detection and Base Load Detection. This module detects events and steady states from the aggregated power profile. It involves also a base load detection procedure, identifying consistent power consumption contributed by appliances operating in a steady state. The detection of steady states isolates periods with minimal power variation. Edge detection identifies significant changes (edges) in the aggregated power profile, potentially indicating appliance events.

Module 2: State Probabilities Update. If an edge is detected, then it is updated the state probabilities for each appliance based on: the magnitude of the edge, the previous state probabilities, and additional information like transition probabilities (if available). However, it is also important to take into account the possibility that the detected edge could be caused by an unknown load, which refers to a non-monitored appliance present in the building

Module 3: State Probabilities Tuning. In this phase, the framework combines information on the updated state probabilities with the total matching criterion and the Switch Continuity Principle, to finely tune the state probabilities. This step involves an optimization algorithm that takes into account above mentioned criteria. After this phase, one of the states of each appliance will have a probability near 1 and the other probabilities near zero.

In practical scenarios, load meter measurements are prone to the presence of sensor noise, transient spikes, and signal fluctuations around the mean operating power of an appliance. The edge detection algorithm starts by identifying if the system is likely to be in a steady state considering the power grid noise σ_g^2 variance. Therefore, if the absolute value of the difference between the current and the previous steady states is greater than σ_g, we consider that a new edge E is detected.

Accurate estimation of the base load is also important for enhancing the accuracy of NILM algorithms, particularly those employing state-based approaches. The base load represents the consistent electrical consumption of appliances operating in a steady state. By accurately characterizing the base load, algorithms can effectively differentiate it from appliance-specific states, improving the overall performance of NILM systems. In this work, the base load is estimated by a novel proposed online algorithm.

The active power states of FSM (Fig. 12) appliances cannot be considered constants. The active power can fluctuate due to changes in the supply voltage and variations in load impedance. Here is proposed a log transformation in order to represent the transformed active power with a Gaussian distribution and remove the dependency of the power variance with the expected. This is important to estimate the likelihood of observing a detected edge E(t) given a power transition in load i from state j to state k. In order to be realistic, it is considered that unknown loads could exist in the building, and therefore, it could be the case that the change E(t) is due to an unknown state transition and not due to a transition in the state of any of the N monitored appliances. In order to assign a likelihood of the unknown transition, this work exploits the idea of an improper constant density over the whole Euclidean which is often used in outliers clustering.

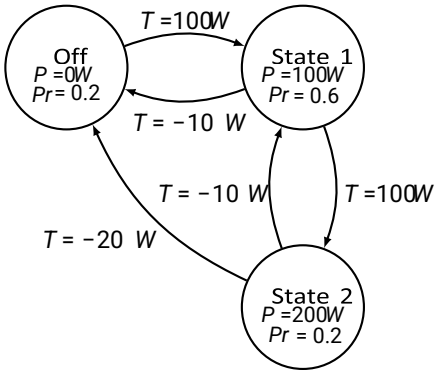

Fig. 12: Finite State Machine Model. The diagram shows the appliance states (Off, State 1, State 2) with their respective power consumption (in Watts, W) and the probability (Pr) of being in that state at a given time t. Transitions between states are labeled with power differences (T) in Watts

After updating the probabilities of different appliance states, there often remains uncertainty, meaning that an appliance might still be associated with multiple states with varying probabilities. The aim of the State Probabilities Tuning step is to converge toward a solution where each appliance adopts a singular state with a probability near 1. It is also an opportunity to use criteria not employed in the steps before, like the Total Matching Criterion, and also consider the possibility of more than one state transition. We propose the use of a modified Population-Based Incremental Learning algorithm (PBIL) for this step. It is important to note, that the PBIL algorithm starts from a probability vector that is partially converged, and so, the running time up to convergence is expected to be lower. Also, this is important because solutions with a high fitness function but far from the real behavior of the appliances, are less probable to be sampled from the converged probability vector, thus, improving the robustness of the method. In that sense, the connection between the State Probabilities Update and State Probabilities Tuning phases not only improves computational efficiency but also the robustness of the method. This work is in the phase of preparing a journal publication to be submitted to the IEEE TRANSACTIONS ON SMART GRID journal.

3.3.3. Contribution to the WP objectives

The obtained results contribute significantly to the objectives outlined in the workpackage. Let's break down how each result aligns with these objectives.

The first result involves proposing and evaluating a multi-objective formulation for parameter identification in photovoltaic modules, which enhances the accuracy and reliability of diagnosing photovoltaic systems. This directly relates to the workpackage objectives in several ways:

New Ways of Using Electric Energy (ESS and Consumption Strategies): By accurately diagnosing the parameters of photovoltaic modules, it becomes possible to optimize the energy storage and consumption strategies based on real-time data, ensuring efficient utilization of solar energy.

Engaging Customers in Energy Applications: If customers can see the tangible benefits of accurate parameter diagnosis in terms of optimized energy usage and reduced costs, they are more likely to engage in energy-saving practices.

The second results involve proposing a Double-Single Diode Model (D-SDM) for parameters identification in non-uniform operating conditions. The proposed D-SDM method for reliable characterization under non-uniform operating conditions also aligns with the workpackage objectives:

New Ways of Using Electric Energy (ESS and Consumption Strategies): Characterizing photovoltaic modules accurately under varying conditions is essential for designing effective energy storage and consumption strategies that adapt to different irradiance scenarios.

Engaging Customers in Energy Applications: When customers observe consistent performance and reliable energy generation estimates, they are more likely to trust and engage with energy applications.

The third result involve a Real-time NILM Technique for Low-Frequency Sampling. The proposed real-time framework for NILM also contributes to the workpackage objectives:

New Ways of Using Electric Energy (ESS and Consumption Strategies): The real-time framework allows for more immediate responses to energy consumption events, enabling more effective energy storage and consumption strategies.

Reducing Energy Consumption (Smart Meters): By providing real-time insights into energy consumption events, the framework complements smart meters in identifying consumption patterns and optimizing energy usage.

Engaging Customers in Energy Applications: Real-time feedback on energy consumption events can engage customers by helping them understand their energy usage patterns and make informed decisions.

3.3.4. Scientific achievements

Publication

#	Title, incl. citation information	Type (Conference, journal, book chapter)	Status (Submitted, accepted, published)	DOI
1	**Identification of static and dynamic parameters of PV models through multi-objective optimization**, in 2023 IEEE 17th International Conference on Compatibility, Power Electronics and Power Engineering (CPE-POWERENG)	Conference paper	published	https://doi.org/10.1109/cpe-powereng58103.2023.10227400
2	**Challenges in photovoltaic parameter identification under mismatching conditions**, in IEEE International Conference on Clean Electrical Power (ICCEP), 2023	Conference paper	published	Not online yet
3	**Dynamic modeling of si-based photovoltaic modules using impedance spectroscopy technique**, in IEEE International Conference on Clean Electrical Power (ICCEP), 2023	Conference paper	published	Not online yet

4. Conclusions

From the scientific point of view WP4, relevant tasks have been undertaken towards WP4 objectives. Work has been done in developing the energy router supervisor, a critical component for controlling residential energy flow. The dynamic simulation model adapts load profiles based on seasonal changes, occupancy levels, and weather conditions. pioneering research introduced a modulation strategy for power converter topologies, enabling full-range soft-switching, minimizing losses, and enhancing adaptability. Multi-Objective Formulation for Photovoltaic Module Parameter Identification, Double-Single Diode Model for Parameter Identification, and Real-Time NILM Technique for Low-Frequency Sampling allowed to enhance energy storage, system adaptability, and customer engagement.

ESR09's journey was not without challenges, including the contract termination of the initial candidate due to trial period issues, resulting in a temporary pause in progress. However, with a successful second recruitment in May 2023, a positive shift occurred, as the new ESR excelled in research and application context definition, demonstrating diligence and commitment. ESR10's achievements are noteworthy, encompassing 8 IEEE conference papers, active workshop participation, a contribution to a book chapter, and a journal paper currently under review. However, activities briefly halted in June 2023 at the employee's request. ESR11's research significantly advances work package goals through three key outcomes: Despite recruitment delays linked to a VISA issue, ESR11 initiated research promptly, focusing on smart building energy optimization and consumer behaviour, with preliminary findings shared through conference papers.

5. References

[1] J. Aguilar, A. Garces-Jimenez, M. D. R-Moreno and R. García, "A systematic literature review on the use of artificial intelligence in energy self-management in smart buildings," Renewable and Sustainable Energy Reviews, vol. 151, p. 111530, 2021.

[2] R. K. Bonthu, H. Pham, R. P. Aguilera and Q. P. Ha, "Minimization of building energy cost by optimally managing PV and battery energy storage systems," pp. 1-6, 2017.

[3] D. Thomas, O. Deblecker and C. S. Ioakimidis, "Optimal operation of an energy management system for a grid-connected smart building considering photovoltaics' uncertainty and stochastic electric vehicles' driving schedule," Applied Energy, vol. 210, pp. 1188-1206, 2018.

[4] J. Froehlich, E. Larson, S. Gupta, G. Cohn, M. Reynolds and S. Patel, "Disaggregated End-Use Energy Sensing for the Smart Grid," IEEE Pervasive Computing, vol. 10, pp. 28-39, 2011.

[5] L. E. Garcia-Marrero, R. A. Guejia-Burbano, G. Petrone, M. Piliougine and E. Monmasson, "Identification of static and dynamic parameters of PV models through multi-objective optimization," in 2023 IEEE 17th International Conference on Compatibility, Power Electronics and Power Engineering (CPE-POWERENG), 2023.

[6] R. A. Guejia-Burbano, G. Petrone and M. Piliougine, "Impedance Spectroscopy for Diagnosis of Photovoltaic Modules Under Outdoor Conditions," IEEE Journal of Photovoltaics, vol. 12, pp. 1503-1512, 2022.

[7] L. E. Garcia-Marrero, M. Piliougine, G. Petrone, M. D. Riso, P. Guerriero and E. Monmasson, "Challenges in photovoltaic parameter identification under mismatching conditions," in IEEE International Conference on Clean Electrical Power (ICCEP), 2023.

[8] M. D. Riso, I. Matacena, P. Guerriero, S. Daliento, L. E. Garcia-Marrero and G. Petrone, "Dynamic Modeling of Si-based Photovoltaic Modules using Impedance Spectroscopy Technique," in IEEE International Conference on Clean Electrical Power (ICCEP), 2023.

[9] S. Baluja, Population-based incremental learning: A method for integrating genetic search based function optimization and competitive learning, School of Computer Science, Carnegie Mellon University Pittsburgh, PA, 1994.

[11] Emiliani, P.; Blinov, A.; Peftitsis, D.; Giannakis, A.; Vinnikov, D. (2022). Reactive Power Control for Bidirectional Isolated High-Frequency Link Converter. 2022 International Symposium on Power Electronics, Electrical Drives, Automation and Motion, SPEEDAM 2022. IEEE, 372–376.

[12] Emiliani, P.; Blinov, A.; Chub, A.; De Carne, G.; Vinnikov, D. (2022). DC Grid Interface Converter based on Three-Phase Isolated Matrix Topology with Phase-Shift Modulation. IEEE 13th International Symposium on Power Electronics for Distributed Generation Systems (PEDG): Kiel, Germany, 26-29 June 2022. IEEE, 1–6.

[13] Emiliani, P.; Blinov, A.; Chub, A.; De Carne, G.; Vinnikov, D. (2022). Black Start and Fault Tolerant Operation of Isolated Matrix Converters for dc Microgrids. 48th Annual Conference of the Industrial Electronics Society (IECON 2022): Brussels, Belgium, 17-20 October 2022. IEEE, 1–5

[14] Verbytskyi, I.; Blinov, A.; Emiliani, P.; Galkin, I. (2022). Digital Control of PFC Rectifier with Combined Feedforward and PI Regulator. 48th Annual Conference of the Industrial Electronics Society, IECON 2022: 48th Annual Conference of the IEEE Industrial Electronics Society. IEEE

[15] Arena, Gabriele; Emiliani, Pietro; Chub, Andrii; Vinnikov, Dmitri; De Carne, Giovanni (2023). DC Fast Charging of Electric Vehicles: A Review on Architecture and Power Conversion Technology. 2023 IEEE 17th International Conference on Compatibility, Power Electronics and Power Engineering (CPE-POWERENG), Tallinn, Estonia, Jun. 14-16, 2023.

[16] Pietro Emiliani, Andrei Blinov, Giovanni De Carne, Gabriele Arena, and Dmitri Vinnikov (2023). Predictive Control for Isolated Matrix Rectifier Without Current Distortion at Sector Boundary. 2023 IEEE 17th International Conference on Compatibility, Power Electronics and Power Engineering (CPE-POWERENG), Tallinn, Estonia, Jun. 14-16, 2023.

[17] Parham Mohseni, Pietro Emiliani, Oleksandr Husev, Dmitri Vinnikov, and Laurens Mackay (2023). A Comparison between Three-Phase Conventional Two-Stage AC-DC and Single-Stage Matrix Converter Approaches. 2023 IEEE 17th International Conference on Compatibility, Power Electronics and Power Engineering (CPE-POWERENG), Tallinn, Estonia, Jun. 14-16, 2023

[18] Pietro Emiliani, Andrei Blinov, Giovanni De Carne, Gabriele Arena, and Dmitri Vinnikov (2023). Three-Phase Four Wire High-Frequency Link Converter for Residential DC Grids. 2023 IEEE 17th International Conference on Compatibility, Power Electronics and Power Engineering (CPE-POWERENG), Tallinn, Estonia, Jun. 14-16, 2023.

[20] Blinov, A.; Roasto, I.; Chub, A.; Emiliani, P.; Vinnikov, D. (2023). Electric Power Management and Control in DC Buildings — State-Of-The-Art and Emerging Technologies. In: Power Quality: Infrastructures and Control. (67–96). Springer. (Studies in Infrastructure and Control).